B. Poletanovic, J. Dragas, I. Ignjatovic, M. Komljenovic, I. Merta, Physical and mechanical properties of hemp fibre reinforced alkali-activated fly ash and fly ash/slag mortars, Construction and Building Materials, Volume 259, 2020, 119677, ISSN 0950-0618,

https://doi.org/10.1016/j.conbuildmat.2020.119677

*Title page

Physical and mechanical properties of hemp fibre reinforced alkali-activated fly ash and fly ash/slag mortars

Bojan Poletanovic[1], Jelena Dragas[2], Ivan Ignjatovic[2], Miroslav Komljenovic[3], Ildiko Merta[1]

[1] Institute of Material Technology, Building Physics, and Building Ecology, Faculty of Civil Engineering, TU Wien, 1040 Vienna, Austria

[2] Faculty of Civil Engineering, University of Belgrade, 11000 Belgrade, Serbia

[3] Institute for Multidisciplinary Research, University of Belgrade, 11030 Belgrade, Serbia

corresponding author: bojan.poletanovic@tuwien.ac.at

Highlights:

- Two hemp fibre alkali-activated mortars (fly ash and fly ash+slag based) were examined.
- The addition of fibres, decrease the density and flexural strength, increase the water absorption rate and compressive strength.
- Significant increase in energy absorption capacity under flexure with increasing fibre dosage.
- The initially more brittle matrix exhibited significantly higher relative toughness increase.

1. Introduction

The construction industry is one of the largest sectors in the world contributing 23% (5.7 billion tons in 2009) of the total carbon dioxide (CO_2) emissions produced by the global economics activities [1]. Because of its huge impact, intensive efforts are directed toward the development and use of regenerative construction design approaches along with a new generation of sustainable, low embodied carbon building materials [2] in order to overcome the traditional *take-make-dispose* model.

Concrete is the most used building material on Earth. The production of concrete leads to large raw resources consumption, high-energy demands and high pollution. The production of Portland cement, as one of the main components of concrete, has a vast carbon footprint. Approximately one ton of CO_2 is released for each ton of Portland cement clinker produced [3]. In order to improve the overall environmental performance of concrete the amount of cement should be reduced (or completely replaced) with less resource-demanding materials (e.g. industrial by-products such as ashes, slags) [4-5].

Alkali-activated (AA) binder is so far the most commonly researched alternative to the traditional cement-based binder in the past decade. In AA materials, different natural and waste materials are activated using various alkaline solutions. Waste material that is greatly used in the production of AA binder is fly ash, which is thermal power plant coal combustion residue. It can be used as the only solid prime material within AA binder or in combination with ground granulated blast furnace slag (GGBFS) [6–10]. Available research results show that both types of previously mentioned AA binders can provide adequate mechanical properties for structural concrete if properly designed and cured [9, 11–13]. Based on the AA product formed after the activation of the solid prime materials, two different categories can be defined [14]: i) calcium silicate hydrate gel; ii) alkaline alumino-silicate hydrate gel (also known as inorganic or geopolymer gel). In the following, both terminologies, i.e. AA binder and geopolymer will be used, according to the naming used in the cited literature.

Alkali-activated mortars, similarly as cement-based mortars, are so-called quasi-brittle materials, which have low crack resistance and reduced energy absorption capacity under tensile load. The incorporation of fibre reinforcement into the matrix significantly reduces these deficiencies of the composite shifting its behaviour toward quasi-ductile or even ductile one with significantly improved energy absorption capacity in the post-peak region of the stress-strain curve [15–17]. The common fibre reinforcement in AA mortars (like in cement-based mortars) are made from steel, synthetic or glass [18–20]. These fibres are highly dependent on virgin material resources and are extremely resource and energy-intensive to manufacture.

Due to the growing environmental awareness natural plant-based fibres, such as hemp, coir, flax, sisal, jute, cotton, etc. have been recently increasingly considered as a possible sustainable substituent for traditional fibres in cementitious matrices [21–29]. Because of their low price, worldwide availability, biodegradability, renewability, small energy consumption during their production, positive environmental impact, natural fibres are becoming more and more attractive [21, 28, 30, 31]. Natural fibres could be a viable replacement for synthetic (micro and macro) fibres since they have similar geometry, tensile strength and modulus of elasticity. The properties of the most common natural fibres are listed in Table 1.

Table 1. The physical and mechanical characteristics of natural fibres [32-36]

Fibre plant origin	**Fibre diameter [µm]**	**Tensile strength [MPa]**	**Elastic Modulus [GPa]**	**Elongation at failure [%]**
Abaca	18	400-980	6.2-20.0	1.0-10
Bamboo	12-30	140-800	11.0-32.0	2.5-3.7
Coir	10-460	95-230	2.8-6.0	15.0-51.4
Cotton	10-45	287-800	5.5-12.6	3.0-10.0
Flax	12-600	343-2000	27.6-103.0	1.2-3.3
Hemp	8-600	270-900	23.5-90	1-3.5
Jute	20-200	320-800	30	1.0-1.8

Luffa Cylindrical	200	385	12.2	2.65
Pineapple leaf	50	180-1627	1.44-82.5	1.6-14.5
Raffia	5	148-600	12.3-36	2.0-4.0
Sisal	8-200	363-700	9.0-38.0	2.0-7.0
Wool	18-35	160-240	2.0-3.5	0.8

One of the major challenges in the application of natural fibre composites is still the assurance of their long-term performance (durability). In the alkaline environment of cement-based or AA matrices, natural fibres are exposed to i) alkaline attack and ii) fibre mineralization. In the first case, natural fibres could degrade as a consequence of dissolving of lignin and hemicellulose in the middle lamella of the fibre through the alkaline pore water and of alkaline hydrolysis of cellulose molecules (degradation of molecular chains). In the second case, mineralization is caused by migration of calcium hydroxide toward fibre walls and into the fibre's lumen [23, 37-44]. As a consequence, the composite may undergo strength reduction and loss of toughness (overall embrittlement). The most effective way of mitigation of the natural fibres degradation in the alkaline environment is the fibre surface protection (with sodium hydroxide, hornification, etc.) and decrease of matrix alkalinity [45].

Table 2. Overview of published work dealing with AA materials reinforced with natural fibres

Fibres' type	Fibres' plant origin	Fibres' dosage [wt%]	Fibres' length [mm]	Solid binders	References
short	Coconut	1	30-50	Fly ash	[46]
	Coir	1	3		[47]
	Cotton	1	10; 30		[47–49]
	Raffia	1	3		[47]
	Sweet sorghum bagasse	1; 2; 3	0-50		[50]
	Bamboo	5	0-40	Metakaolin	[51]
	Pineapple leaf	3*	25		[52]
	Sisal	3*	25		[52]
aligned	Abaca	1	the entire length of the sample	Fly ash	[53]
	Cotton	4.5; 6.2; 8.3			[54,55]
	Flax	4.1			[56,57]
	Corn husk	n/a		Metakaolin	[58]
	Curaua	10			[59]
	Jute	n/a; 10			[60]
	Luffa Cylindrical	10*			[61]
	Sisal	10			[59]
	Flax	4; 7; 10		Dehydroxylated halloysite	[62]
	Wool	n/a			[63]

wt% = weight percentage; * in volume percentage (vol%); n/a = information not available

For optimal final mechanical properties of natural fibres composites a well-chosen fibre length and dosage, their good dispersion within the matrix as well as an optimal fibre-matrix bond is crucial. Very limited research work is published dealing with AA materials reinforced with natural fibres (Table 2) and in following their main findings are summarized.

Generally, with the addition of natural fibres the composites porosity increases. This is the result on one side of the fibres' porous structure and on the other side of the air entrapped during mixing. With increased porosity the density of AA composite decreases and consequently its water absorption capacity increases [49, 50, 55].

In case of compression strength of natural fibre reinforced AA matrices (pastes) an interesting different trend than in cementitious composites were reported. With the addition of lower dosages of natural fibres (≤1.0 vol% or wt%), the compressive strength of the composite generally increases [48] and only at higher dosages (≥1.0%) it starts to decrease [47, 50, 51]. In the case of flexural strength under lower fibre

reinforcement dosages (0.5 wt%), it was reported that the AA pastes' flexural strength increases whereas with a further increase of fibre dosage (to 1.0 wt%) the flexural strength starts to decrease [49]. Chen et al. [50] reported an increase in flexural strength even under much higher fibre dosages (up to 2%) and first at 3% fibre dosage the flexural strength started to decrease.

However, the most relevant contribution of fibre reinforcement generally is in the significant improvement of the energy absorption capacity of the material under tensile-, flexural- or impact load. Alomayri et al. [49] showed that if fly ash-based geopolymer pastes were reinforced with 10-mm long cotton fibres in a dosage of 0.5 wt% the toughness of the material under flexural bending (three-point bending test) increased for 60%. At a higher dosage (0.7 wt% and 1 wt%) a pure dispersion of fibres within the matrix and consequently decrease in toughness were observed. Chen et al. [50] in contrary reported that reinforcing fly ash-based geopolymer pastes with 1%, 2% and 3% (to the mass of fly ash) of sweet sorghum short (less than 5 cm) fibres improved significantly the post-peak toughness of the matrix under splitting tensile load, i.e. for up to 1100%, 1600% and 700% respectively. In terms of impact strength, it is shown that reinforcement of fly ash-based AA pastes with both short and aligned cotton fibres significantly improves the characteristics of the material [48, 54, 64].

The predominant part of the published research work is focusing on reinforcing AA matrices with bundles of longitudinal aligned natural fibres and not on short discrete fibre reinforcement. Yet, these composites by definition do not belong to the category of so-called fibre-reinforced composites [15] containing randomly distributed short discrete fibre-reinforcement within the matrix. There is a significant difference in the reinforcing mechanisms of the two reinforcement types, in their effect on the matrix and consequently in the final properties of the composite itself.

Additionally, all the literature is focusing on matrices based solely on natural fibre AA pastes not containing any (fine or coarse) aggregate. Yet, due to their limited mechanical characteristics and high costs generally pastes (either cement-based or alkali-activated) could not be considered as potential building materials in civil engineering applications. In order to be a possible replacement for traditional fibre reinforced concrete, i.e. in applications where high energy absorption capacity, resistance to impact- and dynamic loading or prevention of cracking is required (industrial floors, columns hinge area, tunnel lining, shotcrete application, etc.), fibre reinforced AA pastes should inevitably contain aggregate also.

Motivated by this lack, this research is a first "upscale" of natural fibre AA pastes toward the development of potential building material by incorporating fine aggregate (0.0-4.0 mm) into the AA paste. In such a way natural fibre AA mortars were obtained which with the gradual addition of coarse aggregate could be further upscaled toward natural fibre AA concretes.

As reinforcement fibres of industrial hemp (Cannabis Sativa L) were selected, on one side since they are the most widely available natural fibres in the category of microfibres, are widely used as fibre reinforcement in cementitious composites, had a long tradition in Europe, are recently increasingly recultivated, revitalized and becoming locally available, and on the other side because there is still no work published (Table 2) on hemp fibre reinforced AA matrices [65].

Two groups of AA mortars based on different solid prime materials, i.e.: i) fly ash and ii) a combination of fly ash and ground granulated blast furnace slag (GGBFS) were used. So far there is no research published dealing with fly ash/GGBFS systems reinforced with natural fibres. As fibre reinforcement short discrete hemp fibres (dosages of 0.5 vol% and 1.0 vol%) were used and the mortars physical- and mechanical properties in term of the density, water absorption, compression- and flexural strength, as well as its energy absorption capacity under flexure experimentally evaluated. Additionally the composites microstructure and the fibre/matrix interaction under scanning electron microscopy (SEM) were analyzed.

2. Experimental methods

2.1. Materials

The AA mortars tested in this study were made with locally available fly ash ("Nikola Tesla B" power plant in Obrenovac, Serbia) and GGBFS from pig iron production at the facility "Železara Smederevo" (Serbia). Two different samples of fly ash (F1 and F2), which are both by-products of lignite based coal combustion, were collected from the power plant and used without further treatment and GGBFS was additionally grounded to its specific surface area of 400 m²/kg (according to the Blaine test). The chemical composition

of used fly ash and GGBFS samples was determined by X-ray fluorescence analysis and are shown in Table 3. As can be seen, both fly ash samples satisfy the ASTM-C618 [66] criteria for class F fly ash: $SiO_2+Al_2O_3+Fe_2O_3 > 70\%$ and loss on ignition–LOI < 6% with similar chemical composition. The size distribution of fly ash and GGBFS samples was tested using the Malvern Instruments Mastersizer 2000 and presented in Figure 1, whereas the specific gravity was determined according to EN 450-1 (CEN 2012) [67]. The average mean particle size of F1 and F2 was 16.78 µm and 3.98 µm respectively whereas GGBFS 15.49 µm. The density of the two fly ashes F1 and F2 is in the same range, i.e. 1960 kg/m^3 and 2075 kg/m^3 respectively, whereas the GGBFS is much higher 2880 kg/m^3.

Table 3. The chemical composition of fly ashes (F1 and F2) and GGBFS

	SiO_2 (%)	Al_2O_3 (%)	Fe_2O_3 (%)	CaO (%)	SO_3 (%)	Na_2O (%)	K_2O (%)	MgO (%)	LOI (%)
F1	57.38	18.47	5.89	10.05	1.48	0.53	1.89	1.58	1.65
F2	61.14	19.22	4.35	8.32	2.21	0.36	0.66	0.01	4.68
GGBFS	39.88	6.68	0.97	39.34	0.20	0.42	0.61	8.61	1.23

*the percentage of oxides within the corresponding material was given by mass (wt%);
LOI – loss on ignition at 1000 ^oC.

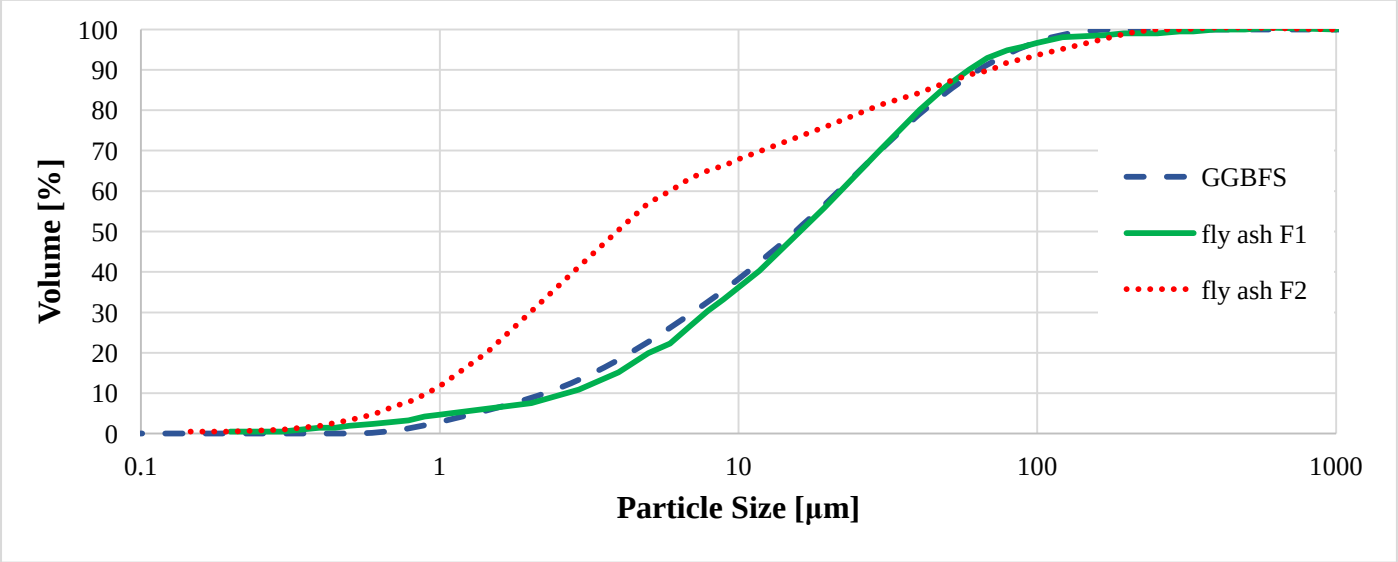

Figure 1. The cumulative particle size distribution of a) fly ash F1, b) fly ash F2 and c) GGBFS

AA mortars were prepared with commercially available sodium silicate solution (28.08 wt% of SiO_2 and 14.7 wt% of Na_2O) from Serbia. Sodium silicate solution had a module of $n=SiO_2/Na_2O=1.91$ and a density of 1514 kg/m^3. The aggregate used in mortar preparation was river sand with water absorption of 0.385% and dry density of 2670 kg/m^3. The particle size distribution of sand is given in Table 4.

Table 4. The particle size distribution of sand

Sieve size [mm]	0.125	0.25	0.50	1.00	2.00	4.00	8.00
Passing [%]	2.19	20.31	51.06	61.38	74.38	97.31	100.00

In this research, primary bast hemp fibres (*Cannabis sativa L*) with a diameter of 8–60 µm cultivated and processed (through the retting process) in Hungary were used (Figure 2). Hemp fibres consist mainly of cellulose (74.4%), hemicellulose (17.9%), lignin (3.7%), pectin (0.9%) and wax (0.8%) [33, 68]. The density of the fibres was 1500 kg/m^3 and they absorb water nearly in 2.5 times of their weight. The tensile strength of hemp fibres varies significantly since it depends on the fibres cross-section, humidity, harvesting time, etc. It is reported to be between 270-900 MPa [33].

Figure 2. Bundle of hemp fibres (left) and hemp fibre image under a scanning electron microscope (right)

2.2. Mortar mix design

For the AA mortar matrices, two different types of mix designs (Table 5) in terms of density and compressive strength were prepared. The amount of the activator to the solid prime material (i.e. 10.0 wt% Na_2O with respect to the solid prime material mass) was chosen based on the trial mixtures testing according to the work given in Komljenovic et al. [69]. The first group of mortar mixture (denoted with FA1) was made only from fly ash type F1, whereas the second one (denoted with FA2S) with the combination of the finer fly ash type F2 and GGBFS (Table 5). The amount of water in the mortar was determined based on the similar workability between the two mortar mixtures and on the additional water needed for the fibres' uptake.

The dry hemp fibres were cut from a bundle of 10 mm in length, separated by hand before mixing and added to the mortar matrix in two different dosages, i.e. 0.5 vol% and 1.0 vol% (volumetric percent). The two dosages were chosen as optimal values for a compromise between mechanical properties in the hardened state and fresh state properties such as workability and fibres good dispersion within the matrix. In hemp fibre reinforced mixtures an additional amount of water was added according to their absorption rate. The control (plain non-reinforced) mortar mixtures are denoted with XXX_0 while the hemp fibre reinforced series with XXX_0.5 and XXX_1.0 for 0.5 vol% and 1.0 vol% dosage of fibres respectively (Table 5).

Table 5. Mortars mix design

Notation	Fine aggregate	AA*	Fly ash	GGBFS	Water	Hemp fibres	
	[g]	[g]	[g]	[g]	[g]	[g]	[vol%]
FA1_0	1350	306	450	–	70	–	–
FA1_0.5	1350	306	450	–	70 + 15**	6.25	0.5
FA1_1.0	1350	306	450	–	70 + 30**	12.50	1.0
FA2S_0	1350	306	225	225	50	–	–
FA2S_0.5	1350	306	225	225	50 + 15**	6.25	0.5
FA2S_1.0	1350	306	225	225	50 + 30**	12.50	1.0

*AA-alkali activator; ** Additional water for fibres absorption

2.3. Specimens preparation

Preparation of all mortar specimens was done in standard RILEM-CEM mixer [70]. First, the entire quantity of sodium silicate solution, additional water and fly ash or fly ash and GGBFS were added to the mixer. Then the paste was mixed for about 60 seconds at low speed (140±5 rev/min). Next step is 30 seconds of the rest period, which is used to add sand and dry hemp fibres (followed with additional water for their uptake) in the mixer. The mortar was then mixed for an additional 90 seconds at medium speed (285±10 rev/min). After mixing, mortars were cast into standard prismatic mortar specimens (40×40×160 mm³), vibrated and placed in plastic bags. After approximately one hour at laboratory conditions (temperature of 20 ± 2°C and relative humidity of 50±5%), the specimens were placed in a heating chamber and cured 24 hours at 80°C. After curing at elevated temperatures, specimens were further stored at standard laboratory conditions until testing.

2.4. Experimental campaign

2.4.1. Mineralogical analysis

For mineralogical analysis, bulky mortar specimens after three-point bending tests were crushed to smaller pieces and dried at 60 °C in an oven to the constant weight (for 3 days). The dried, still bulky material was then ground to particle sizes bellow 0.063 mm. Such prepared powders were regarded as analytical samples suitable for measuring X-ray Powder Diffraction (XRD) records.

To study the mineral composition of samples the powder XRD measurement was applied using an automatic theta/theta X-ray diffractometer STOE & Cie GmbH (Germany) in a 2θ range of 5–65°. CuKα radiation and Ni filter were applied. The XRD records were evaluated by the Bede ZDS pre W95/98/NT program. The samples used for XRD measurements were the two different AA pastes used as the matrix by the AA mortars (FA1 and FA2S). The pastes used for XRD analysis have the same water/binder ratio as the AA mortars but contain neither aggregate nor hemp fibres.

2.4.2. Physical properties

The physical properties of the mortars are tested at the 28 days of the specimens' age.

The measurement of the bulk density was conducted on the six mortar prisms (40×40×160 mm³) and the mean value is used as a representative for each mortar group. The bulk density was calculated as follows:

$$D\ [kg/m^3] = M/V \quad (1)$$

where M is the mass of specimens and V is the volume of specimens.

The standard ASTM C20 was adopted to calculate the water absorption. For the water absorption test (Figure 3), six halves of the mortar prism specimens with a dimension of 40×40×80 mm^3 (halves of the specimens after 3PBT) were used. The specimens were immersed in a water bath (supported by a plastic holder on a bottom side in order to provide a contact to water for all surfaces) at room temperature (20 °C) for two days to reach water absorption equilibrium. Afterwards, the mean value is calculated and used as a representative.

The percentage of the water content was determined using the following equation:

$$Mt\ [\%] = (Wt - Wo) \times 100 / Wo \quad (2)$$

where Wt is the weight of water-saturated specimens and Wo is the weight of dry specimens.

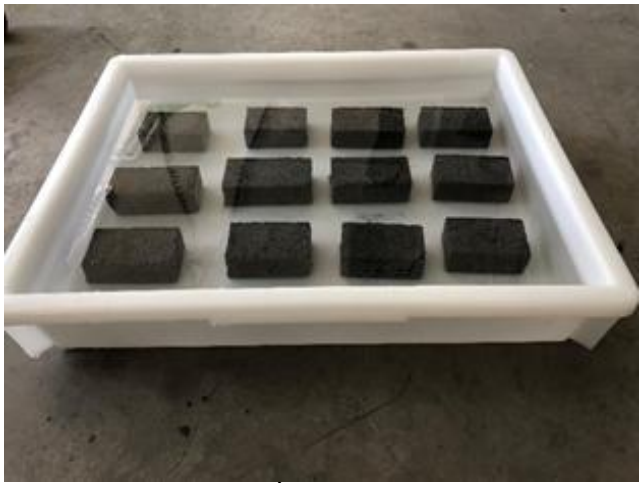

Figure 3. Water absorption testing

2.4.3. Mechanical properties

All mechanical tests were conducted at specimens' age of 28 days. According to the norm ÖNORM EN 1015-11 (2018) [71], three-point bending tests (3PBT) on six identical prisms specimens (dimensions of 40×40×160 mm³) were conducted and on split halves of the specimens compressive tests (on 40×40 mm² area) were done (in summary on 6 halves). The tests were carried out on a mechanical testing machine Zwick/Roell Z250 with a load capacity of 200 kN, rigidity of 8×10^{-3} mm/kN at a room temperature of 21°C and relative humidity of 50%. The 3PBT was performed under controlled displacement of 400 μm/min (closed-loop test) in order to obtain a stable post-peak part of the curves, and compressive test with the loading rate of 0.5 MPa/s (Figure 4).

The peak of the force-displacement (force-mid deflection) curve (Figure 5) represents the specimens' flexural strength whereas the effectiveness of the fibres is represented by the post-peak part of the diagrams. By the definition, the energy absorption capacity (or the toughness) of the composite is the area under the force-displacement curve divided by the specimen's cross-section [72, 73]. Thus, the higher the post-peak branch of the curve, the tougher the composite is, whereas a sudden force drop accompanied with small displacements indicates a highly brittle matrix.

Since during the tests the increment of the specimens' energy absorption capacity beyond a 98% drop of the maximal force was negligible, the upper limit of the integration was chosen at the deflection corresponding to this point.

Figure 4. Three-point bending test (left), and compressive test (right)

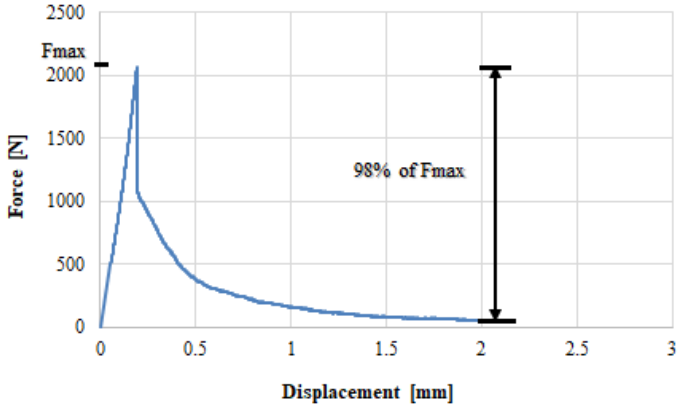

Figure 5. A force-displacement (mid-span deflection) curve after 3PBT of a FA1_1.0 specimen

2.4.4. Microstructural analysis

To investigate the fracture surface of the samples scanning electron microscopy (SEM) VEGA TS 5130 MM, Tescan was used. SEM imaging of the sample surface was performed at an accelerating voltage of 10 kV. In each specimen group, for the SEM analysis, the prism with the flexural strength closest to the mean value was selected. After the 3PBTs (28 days of the specimens' age), the samples for the SEM analysis were taken from the fractured surface of the specimens. The pull-out trace of fibres could be tracked only at the fractured surface. For uniformity, all SEM samples (with and without fibres) have been taken from the fractured surface. For SEM analysis, selected fragments of the samples were immersed in isopropyl alcohol for 24 h and then dried at 50 °C for 2 h. The samples were rinsed in acetone in an ultrasonic bath for 3 min and finally dried in a laboratory oven at 50 °C for 2 h. Prior to SEM analysis, the samples were Au-coated.

3. Results and discussion

3.1. Chemical analysis

In Figure 6 XRD measurements of the two series of AA paste used in this study as matrices for the two AA mortars (FA1 and FA2S) are presented.

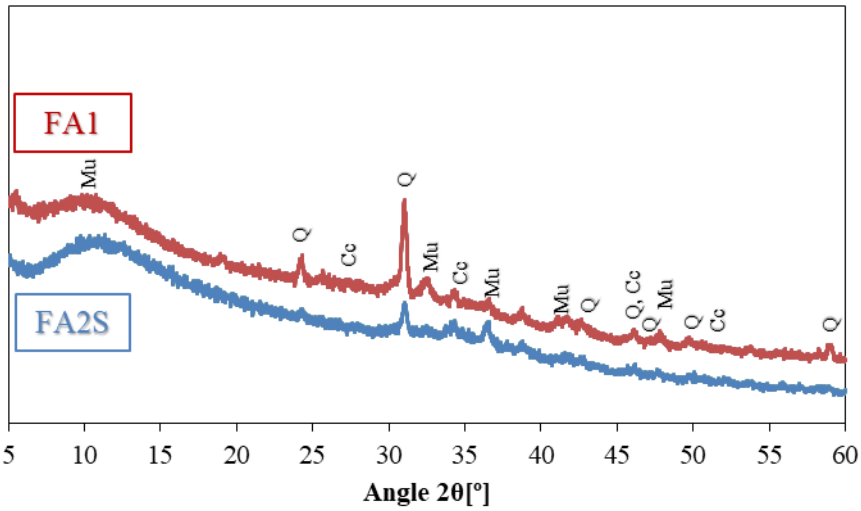

Figure 6. X-ray Powder Diffraction measurements of the FA1- fly ash based AA paste and FA2S- fly ash and GGBFS based AA paste

Both samples (FA1 and FA2S) are specified by the presence of quartz (Q: SiO_2), mainly coming from sand, co-existing with minor minerals mullite (Mu: $Al_6Si_2O_{13}$) coming from fly ash and calcite (CC: $CaCO_3$) which comes as a consequence of the natural carbonation of present calcium. The crystalline character of the FA2S sample is suppressed and approved by the lower diffraction intensities of the identified minerals. This difference is mainly distinguishable at quartz, mainly at 31.342 °2θ. The raised XRD record between 5 and 15° 2θ indicates the occurrence of amorphous products as the result of the proceeded alkali-activated reaction. The FA2S sample shows a larger raised XRD record within 5 and 15 °2θ compared to that of FA1. This indicates that more amorphous products are formed within the sample FA2S than in FA1. The presence of slag in the FA2S matrix contributes to generate more amorphous products and consequently refine the pore structure of the matrix [74]. More amorphous products within the FA2S mortar leads to its more compact structure than in FA1 [75].

Besides, Figure 1 shows that the mortar FA2S has lower particle sizes of the solid prime materials than the mortar FA1 which leads to the more compact structure of the FA2S with lower pores [75], which can be seen in Figure 7.

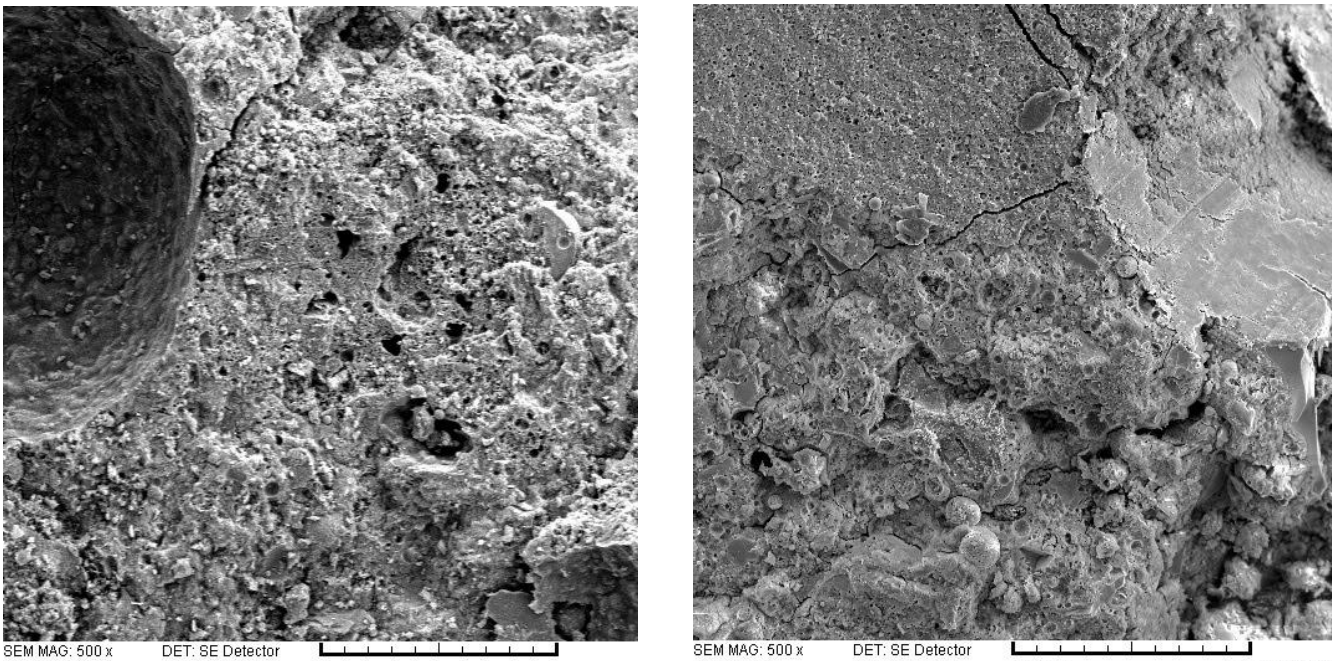

Figure 7. SEM images of non-reinforced FA1-fly ash based AA mortar (left) and FA2S-fly ash and GGBFS based AA mortar (right)

3.2. Physical properties

The measured values of mortar specimens' **bulk densities** are presented in Table 6 with an average value and standard deviation of the results. In the AA fly ash-based specimens (FA1), the mortar's bulk density ranged between 1830–1860 kg/m^3, whereas in AA fly ash and GGBFS-based specimens (FA2S) was on average 14% higher. The higher density of the solid materials (GGBFS and fly ash F2), the higher amount of smaller particles (in range of 1-10 μm, Figure 1) which could fill the spaces between larger particles, and the lower amount of water used in FA2S mixture resulted in denser matrix compared to the FA1.

Table 6. Bulk density average value (with standard deviation) results for FA1-fly ash based AA mortars and FA2S-fly ash and GGBFS AA based mortars

Notation	Bulk density (kg/m^3)
FA1_0	1857.85 (23.9)
FA1_0.5	1832.77 (8.1)
FA1_1.0	1829.46 (11.5)
FA2S_0	2114.96 (22.1)
FA2S_0.5	2074.66 (18.0)
FA2S_1.0	2067.43 (14.4)

With the addition of hemp fibres, a slight decrease in the bulk density of the matrix was observed. In comparison to non-reinforced AA fly ash mortars (FA1) the density of reinforced mortars decreased by 1.34% and 1.53% for 0.5 vol% and 1 vol% of fibre dosage, respectively. A slightly stronger decreasing trend was observed in AA fly ash and GGBFS mortars (FA2S), i.e. in case of 0.5 vol% and 1.0 vol% fibres dosage the density decreased for 1.9% and 2.25%, respectively.

Generally, the decrease in density of fibre reinforced mortars is the result of the higher porosity caused by entrapped air within the matrix during the mixing of fibres. Additionally, the lower density of hemp fibres

itself compared to the density of the AA matrix results in a lower final density of fibre-reinforced composites. However, the density decrease was still within the 5% margin for all tested specimens.

Generally, using natural fires the density of the matrices slightly decreases, regardless of the type of composites. The matrices in the studies of Chen et al. [50] and Alomayri et al. [49] were pure pastes containing no aggregate, the mix design was different, and the additional water needed for fibre absorption was not equally added in all pastes. However, it can be noticed the decreasing density trend after the addition of the short natural fibres to the mixture, as in the conducted present research. Chen et al. [50] used short, sweet sorghum fibres (in a dosage of 1%, 2% and 3% of the fly ash mass) in fly ash-based geopolymer pastes. The density of the plain matrix decreased by 2%, 4% and 7% when reinforced with 1%, 2% and 3% of fibres respectively. Alomayri et al. [49] reported a much more pronounced density decrease by geopolymer paste reinforced with 10-mm long cotton fibres, i.e. 5% and 10% for fibre dosages of 0.5 wt% and 1.0 wt% respectively. In the case of 1.0 wt% fibres dosage, additional water was used to increase the matrix workability that left empty pores after evaporation (during the curing period) and consequently decreased the density of the composite.

The **total water absorption** (mean value and standard deviation) of mortars are shown in Figure 8. The specimens' water absorption capacity could be correlated to the specimens' porosity. Water is able to ingress in open pores that are larger than approximately 1 μm, i.e. opened macropores and large capillary pores. As these occupy the majority of the total pore volume of the material, capturing this range of pores can give a sufficiently accurate estimation of the specimens' total porosity.

As a consequence of the higher compactness of the FA2S matrix compared to FA1 (see Chapter 3.1. Mineralogical analysis) it has about 17% lower water absorption capacity that in turn results in its lower porosity.

In general, the addition of fibres resulted in an increase in the total water absorption of the specimens. It is due to the increased porosity (in range of open macropores and large capillary pores) of the matrix and due to the relatively high water absorption capacity of the fibres itself (2.5 times their weight). The addition of both 0.5 vol% and 1.0 vol% of fibres to the first matrix (FA1) resulted in about 23% higher water absorption compared with non-reinforced specimens. A similar trend was noticed for the second group of specimens (FA2S) where the addition of 0.5 vol% and 1.0 vol% of fibres resulted in 15% and 21% higher water absorption, respectively.

The increase of the fibre dosage (from 0.5 vol% to 1.0 vol%) did not influence significantly the composites total water absorption in neither of the two groups of mortars (FA1 and FA2S), however, they are consistent with the density trend (Table 6).

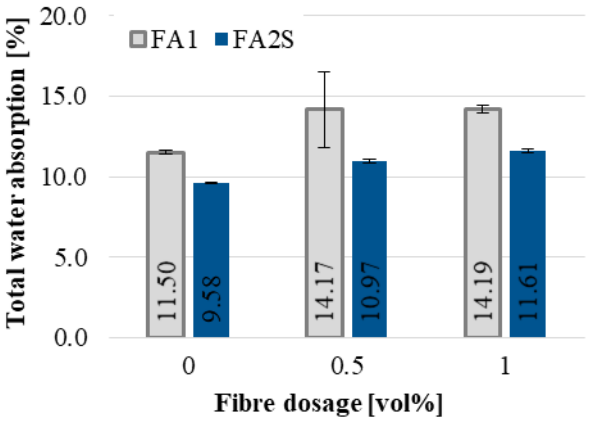

Figure 8. Total water absorption of FA1-fly ash based AA mortars and FA2S-fly ash and GGBFS based AA mortars

Since no results of water absorption of natural fibre reinforced AA materials is published so far in the literature, comparison could be made only with results of cementitious materials reinforced with natural fibres. In these materials, a similar increasing trend in water absorption capacity with the addition of natural fibre reinforcement was reported. In Li et al. [76] the composites water absorption ratio increased by 10%

with the addition of 0.54 wt% of 10-mm long hemp fibres. Page et al. [77] measured water accessible porosity of cementitious mortars through vacuum saturation and obtained approximately 60% higher water absorption by flax fibre reinforced mortars (1.0 wt% fibres, length of 12 mm) than in case of plain mortars.

3.3. Mechanical properties

The **compressive strengths** of both mortar mixtures are presented in Figure 9. The mean value of non-reinforced AA fly ash specimens (FA1) was 21.79 MPa and it was considered as sufficient for low to middle-grade structural application. On the contrary, the second group of non-reinforced mortar specimens (FA2S) had a 48% higher compressive strength (32.24 MPa) compared with the corresponding AA fly ash mortar specimens (FA1). In the FA2S matrix more amorphous products are generated (indicated by XRD results, Figure 6), which refines the pore structure, enhances the compactness of the matrix and improves its compressive strength [74]. This correlates with the obtained higher density of FA2S specimens compared to FA1 specimens (Table 6).

Based on the basic correlation of porosity, density and compression strength of the material it would be expected that with the addition of natural fibres the AA materials compression strength decreases (since the porosity increase and the density decrease), similarly as in the case of natural fibre reinforced cementitious composites are reported [25, 31, 78].

However, in FA2S mortar an interesting, different behaviour was observed. Namely, with the addition of fibres (irrelevant from their dosage), no decrease in compressive strength at all was observed, even a minor increase (i.e 1% and 3% for 0.5 vol% or 1.0 vol% fibres dosage respectively).

In FA1 matrix in case of 0.5 vol% hemp fibres similarly, an unexpected 10% increase in compression strength compared to the plain matrix was observed. Solely in case of 1.0 vol% fibres, a 5% decrease in compression strength occurred.

Based on these results it seems that lower-density matrices (i.e. less compact matrix with a higher ratio of open macropores and large capillary pores) are more sensitive to higher fibre dosages than higher-density matrices (i.e. more compact matrix with a lower ratio of open macropores and large capillary pores) which are able to withstand a strength decrease even at high fibre dosages. It is the result of the fact that the compression strength is predominantly governed by the strength of the matrix itself (resulting from density and porosity) and way less with the effect of fibres itself. Thus as denser the matrix, more pronounced of this effect is.

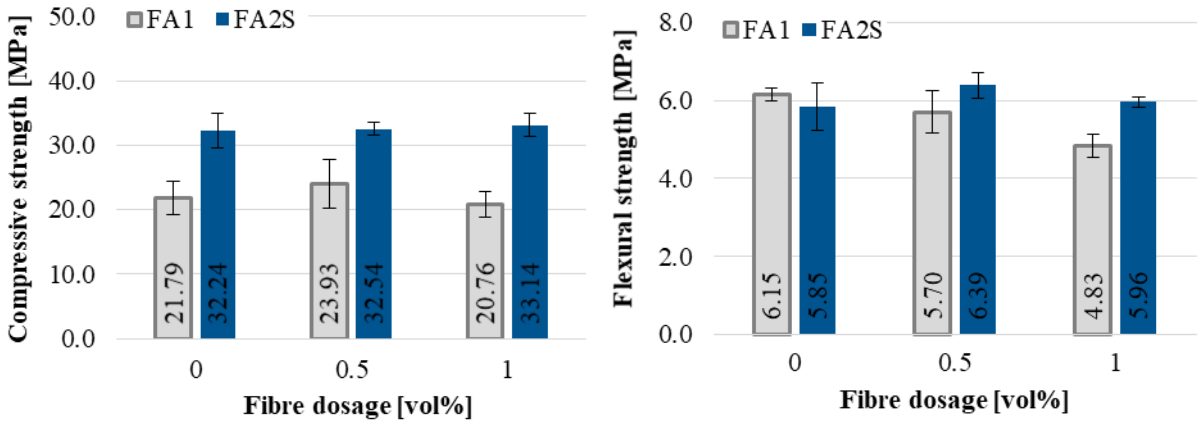

Figure 9. Compressive and flexural strengths of FA1-fly ash based mortars and FA2S-fly ash and GGBFS based AA mortars

A similar trend was reported in the literature for AA pastes reinforced with natural fibres. Alomayri and Low [48] showed that in fly ash-based geopolymer pastes reinforced with cotton fibres (10-mm long and dosage of 0.3, 0.5, 0.7 and 1.0 wt%) first at 0.5 wt% of fibres the compressive strength increased by 140% and then with an increase of fibres dosage (0.7 wt% and 1.0 wt%) the compression strength started to decrease (by 24% and 38% respectively). This was attributed to the agglomeration of fibres resulting in their pure dispersion within the matrix, however, it could be also due to the higher water/binder ratio (namely in matrices with 0.7 wt% and 1.0 wt% a non-specified quantity of additional water was added).

Korniejenko et al. [47] tested fly ash-based geopolymer pastes reinforced with coir-, raffia- and sisal fibres (3-mm long) as well as cotton fibres (30-mm long) and reported about an increase in compression strength even at a relatively high fibre dosage of 1.0 wt%. The compressive strength increased by 27%, 15% and 2% (in case of coir-, cotton-, and sisal fibres respectively), and only in case of raffia fibres, a decrease by 45% was observed. The strength decrease was believed to be the result of the pure cohesiveness between the fibres and the matrix.

In all other works with a higher fibre dosage (≥1%) a decrease in compressive strength was reported. Chen et al. [50] showed that fly ash-based geopolymer pastes decreased the compressive strength by 9%, 17% and 26% when reinforced with short, macro sweet sorghum fibres in dosages of 1%, 2% and 3% (of the fly ash mass) respectively. Sá Ribeiro et al. [51] also reported a decrease of the compressive strength by 50% in metakaolin-based geopolymer pastes reinforced with 5 wt% of bamboo fibres (up to 40 mm in length).

The force-displacement (mid-span deflection) diagrams of the FA1 and FA2S mortar groups under 3PBT are given in Figure 10. The specimens exhibited single cracking visible in the initiation of one discrete crack at the peak and a strain-softening behaviour in the post-peak region. The peak of the curve represents the **flexural strength** of the composite.

FA1

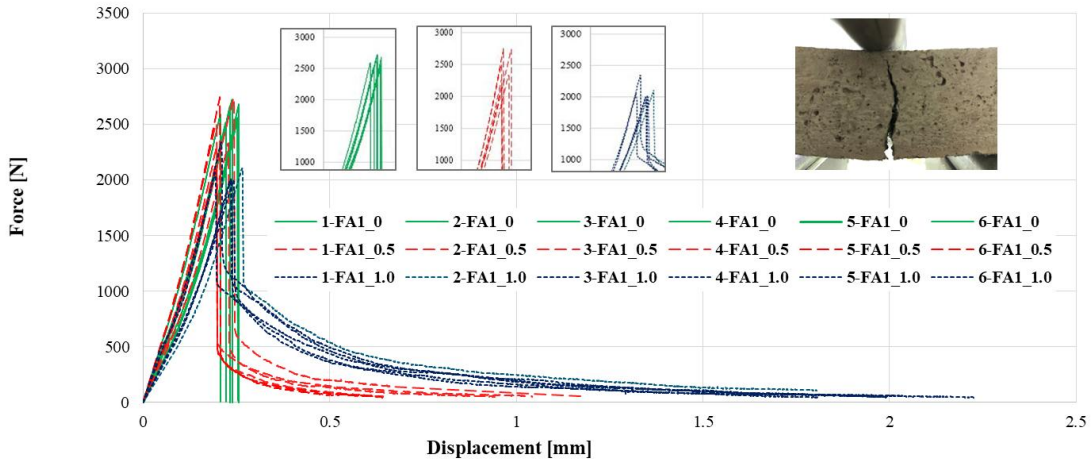

FA2S

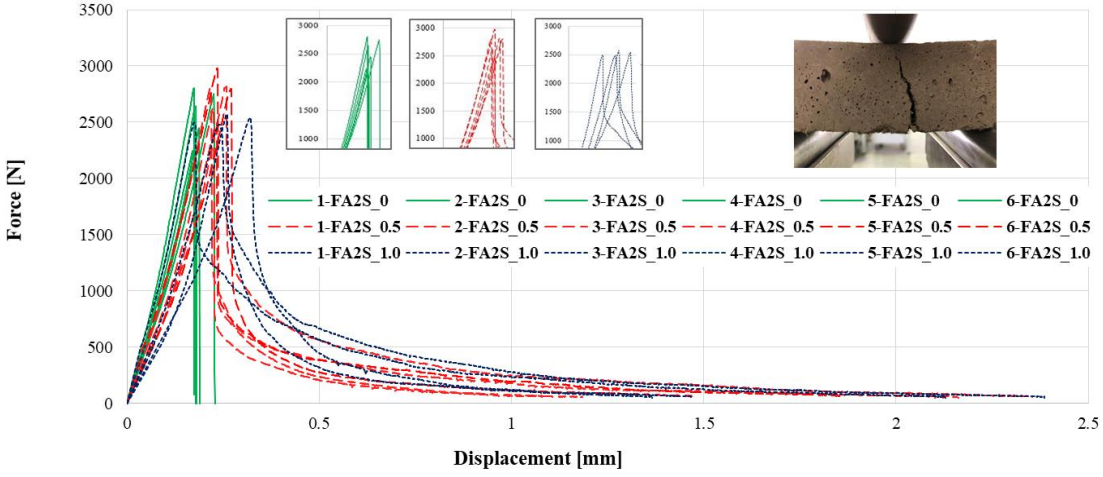

Figure 10. Force-displacement curves under 3PBT of: a) FA1-fly ash based AA mortars (upper) and b) FA2S-fly ash and GGBFS based AA mortars (lower)

Concerning the flexural strength (Figure 9) of non reinforced mortars, it is interesting to note that by the FA1 group the flexural strength is slightly higher (6.15 MPa) than by FA2S (5.85 MPa) although their compression strength is on average 32% lower.

Generally, in fibre reinforced composites, the addition of fibre reinforcement to the matrix does not have a significant influence on the composite's flexural strength since flexural strength is basically determined by the strength of the matrix itself and the fibres becoming active in carrying stresses after the matrix is cracked [15].

With the addition of hemp fibres, the trend of the flexural strength in FA2S mortars follows the trend of their compression strength, i.e. only a slight increase by 9% and 2% in case of 0.5 vol% and 1.0 vol% fibres respectively. Contrary, by FA1 mortars with the increase of fibre dosage, the flexural strength trend differs from trend of their compressive strength and it decreases by 7% and 21% for 0.5 vol% and 1.0 vol% fibre dosages respectively. This indicates that in terms of flexural strength a matrix with a higher density and compactness (such as FA2S) could remain its flexural strengths even at high fibre dosages (1vol%).

In terms of the fibre dosage regarding the flexural strength of the tested composites, the 0.5 vol% seems to be an optimal value. With an increase of the dosage to 1.0 vol%, the flexural strength decreases in both mortar series (FA1 and FA2S).

Alomayri et al. [49] reported a similar trend in flexural strength in fly ash-based geopolymer pastes reinforcement with cotton fibres (length of 10 mm). In the case of 0.5 wt% reinforcement, the flexural strength increased by 12% whereas with the further increase of fibre dosage (to 1.0 wt%) the flexural strength decreased by 1%. Under higher fibre dosages (of sweet sorghum fibres) in fly ash-based geopolymer pastes Chen et al. [50] reported a similar trend in flexural strength. At a 1% and 2% (of fly ash mass) fibre dosages, the flexural strength increased for 34% and 52% respectively, whereas the further increase of the dosage (to 3%) resulted in an 8% decrease of the flexural strength. Sankar et al. [79] reported a 67% increase in flexural strength by metakaolin-based geopolymer pastes when reinforced with 5 wt% bamboo fibres (length 40 mm).

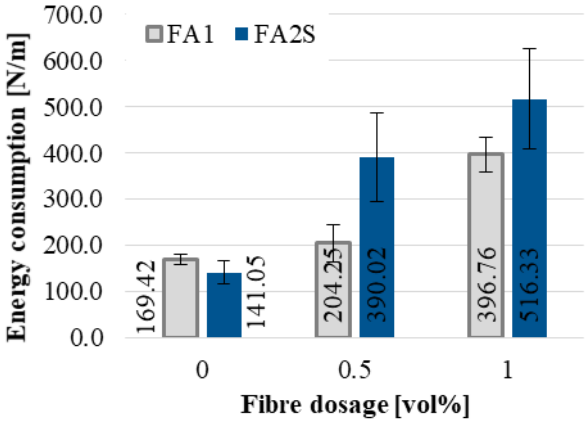

Figure 11. Energy consumption under flexure of FA1-fly ash based AA mortars and FA2S-fly ash and GGBFS based AA mortars

The most relevant contribution of a fibre reinforcement generally is in the significant improvement of the energy absorption capacity (under tensile-, impact load, bending and even under compression) of the plain matrix. Fibres effectively prolong the crack initiation and propagation within the brittle matrix, and in the cracked state of the composite (in the so-called post-peak region), they significantly improve the energy absorption capacity of the material by providing stress transfer through bridging the cracks.

The improvement of the behaviour of the composite in the post-peak region of the force-displacement curves under 3PBT, when reinforced with hemp fibres, could be nicely seen in Figure 10. Plain matrices (series XXX_0) exhibit almost no deformation capacity in the post-peak. After reaching a maximum force a sharp drop of the force in the peak region occurs, indicating a negligible energy absorption capacity (calculated as the area under the curve) of the material. In contrary hemp fibre reinforced mortar matrices (series XXX_0.5 and XXX_1.0) exhibit a significantly higher deformation capacity in the post-peak region, which is apparent from the appearance of a plateau in curves indicating a way higher energy absorption capacity. Thus when reinforced with hemp fibres the deflection capacity of AA mortar specimens is significantly higher than the deflection of plain matrices under the same external load. Or reversely, hemp

fibre reinforced AA mortars are able to carry much higher residual load in the cracked state under the same deflection than non-reinforced matrices. With increasing the hemp fibre content the deflection capacity of mortars increases even further.

The **energy absorption capacity under flexure** (Figure 11) of non-reinforced AA fly ash based mortars (FA1) is 169.43 N/m whereas the GGBFS based mortars (FA2S) have 17% lower values, i.e. 141.05 N/m. This was expected since FA2S is a more brittle matrix (denser and more compact matrix results in a lower level of aggregate/particles interlock which in turn results in lower energy absorption capacity).

However, by reinforcing the matrices with hemp fibres a very interesting significantly different behaviour has been observed, namely, the two matrices showed exactly the opposite characteristics. The more brittle matrix became tougher (than the originally tougher one) independent of the fibre dosage.

With the addition of 0.5 vol% and 1.0 vol% of hemp fibres, the energy absorption capacity of the fly ash-based AA mortars (FA1) (the tougher one) increased solely by 21% and 134%, respectively, whereas by FA2S series (the more brittle matrix) increased significantly more, i.e. by 177% and 266%, respectively. Thus even if the plain FA2S mortar started with 17% lower energy absorption than FA1, after reinforcing it with hemp fibres it exhibited 91% and 30% higher energy absorption capacity compared to FA1 mortar for 0.5 vol% and 1.0 vol% of hemp fibres respectively. In the force-displacement curves (Figure 10) by FA2S composite after the matrix cracked (peak of the curve), the pull out of the fibres in the post-peak region starts much earlier (at 64% and 33% drop of the force for 0.5 vol% and 1.0 vol% of fibres respectively) than by FA1 composite (at 81% and 49% drop of the force for 0.5 vol% and 1.0 vol% of fibres respectively), i.e. a lower force drop is apparent after the peak. This results in a higher plateau of the curves and consequently increased energy absorption capacity of the composite. It seems that the density, porosity and size of the particles within the plain matrix has a more decisive influence on the end-energy absorption capacity of the hemp fibre AA mortar than it would be expected.

Alomayri et al. [49] reported a 60% increase in toughness under flexural bending (three-point bending test) by fly ash-based geopolymer pastes reinforced with 10-mm long cotton fibres (dosage 0.5 wt%), however under a higher dosages (0.7 wt% and 1.0 wt%) a pure fibre dispersion within the matrix and consequently a decrease in toughness occurred. Chen et al. [50] in contrary reported a significant improvement (up to 1100%, 1600% and 700%) of the post-peak toughness of fly ash-based geopolymer pastes under splitting tensile load, when reinforced with 1%, 2% and 3% (to the mass of fly ash) of sweet sorghum fibres respectively.

However, there is no work published where the influence of the matrix density and size of the particles on the toughness of the material is examined. Assaedi et al. [57] reported about 58% increase in toughness of (aligned) flax fibre reinforced (dosage of 4 wt%) fly ash-based AA materials when the dosage of added nano-silica to the matrix was increased from 1.0 wt% to 2.0 wt% and consequently the density of the composite increased (porosity decreased). The reason was believed to be in a higher gel content that in turn improved the interface between fibres and matrix.

Generally in AA fibre reinforced composites [65, 80] similarly as in case of cementitious materials [81] the interfacial stress transfer between the fibres and matrix - and consequently the behaviour of the composite in the post-peak region - is governed by the following three mechanisms: i) chemical bond (adhesion) between fibre and matrix, ii) friction between the fibre and matrix during fibre pull-out from the matrix and sliding within the channel and iii) the resistance provided by the anchorage of fibres (hooks or deformed geometry in case of steel fibres). The first mechanism (chemical bond) is usually a relatively small part of the entire stress transferred and the third one (anchorage) in case of straight fibres such as hemp does not exist. Thus in our case, the main relevant stress transfer mechanism is the **friction** between hemp fibres and AA mortar matrix along with a minor contribution of the **adhesion** (chemical bond) between fibre and matrix.

The two AA mortar matrices FA1 and FA2S differ in the size and density of their constituent particles and consequently in their overall compactness, density and porosity (Figure 7, Table 6, and Figure 8). FA1 contains in average particles of larger sizes (fly ash F1 in an average of 16 μm), is less compact, has a lower density and higher porosity, whereas FA2S has in average particles of smaller sizes (fly ash F2 in average 4 μm and GGBFS in average 15 μm), is more compact, has higher density and lower porosity. As a consequence of this FA2S is generally a more brittle matrix and contains fewer air voids than the FA1 having consequently lower energy absorption capacity (Figure 11).

Since the addition of hemp fibres does not significantly change the density of the matrix itself (Table 6), solely the initial density (and porosity) of the plain AA matrix itself and the fibre/matrix mutual interaction controls the overall energy absorption capacity of the composite.

As a result of the higher compactness of the FA2S matrix and its lower porosity compared to the FA1 matrix, the fibre/matrix interfaces themselves have also a lower porosity (with much lower surface asperity) that in turn results in way more overall fibre/matrix contact points (Figure 12).

The larger number of contact points provide a much larger overall contact area between the hemp fibres and matrix which in turn provides a stronger (we are discussing a general mechanism) fibre/matrix interfacial bonding and stress transfer mechanism. This is apparent in SEM images of fracture surfaces of AA matrices reinforced with 1.0 vol% of hemp fibres (Figure 13). In the case of FA2S composite (Figure 13) a lower fibre/matrix interface porosity with larger overall fibre/matrix contact area and smoother fibre surface (containing smaller matrix particle rests) after pull-out are evident.

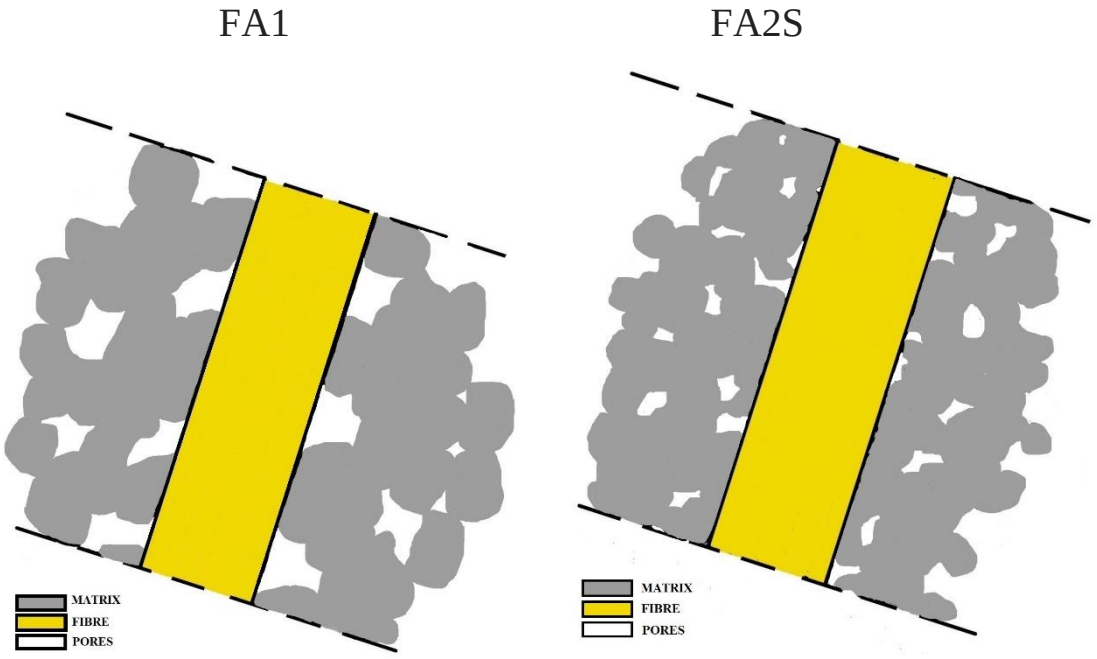

Figure 12. Differences in fibre/matrix interface of the two hemp fibre AA mortars: a) FA1 (fly ash based AA mortar) with higher interface porosity and surface asperity (left); b) FA2S (fly ash and GGBFS based AA mortar) with lower interface porosity and surface asperity (right)

After the interfacial bond strength is reached, de-bonding between fibres and matrix occurs and the fibres are being pulled out from the matrix and are sliding in the matrix channel. In the FA2S matrix, the channels have a smoother surface than in FA1 matrix (Figure 13), however, because of the lower surface asperity, the fibres and the matrix channel are in contact at more asperity points, resulting in more overall contact area between two surfaces which in turn results in a higher overall frictional resistance. This is evident in SEM images, whereas in case of FA2S both the fibres surfaces and the matrix channel surfaces are smoother containing smaller matrix particle-rests after fibre pull-out.

Thus, despite a lower initial energy absorption capacity of the FA2S matrix compared to FA1, after reinforcing it with hemp fibres in FA2S matrix an ideal fibre/matrix interface formed providing a way more optimal bond- and frictional stress transfer with the significantly higher energy absorption capacity of the composite.

FA1 FA2S

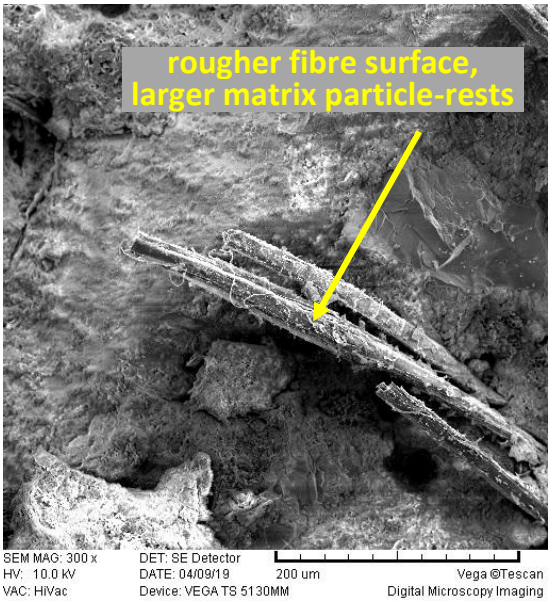
rougher fibre surface,
larger matrix particle-rests
SEM MAG: 300 x
HV: 10.0 kV
VAC: HiVac
DET: SE Detector
DATE: 04/09/19
Device: VEVA TS 5130MM
200 um
Vega ©Tescan
Digital Microscopy Imaging

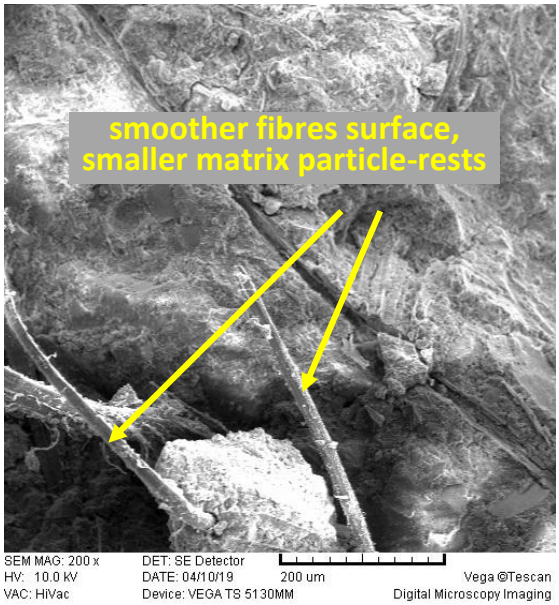
smoother fibres surface,
smaller matrix particle-rests
SEM MAG: 200 x
HV: 10.0 kV
VAC: HiVac
DET: SE Detector
DATE: 04/10/19
Device: VEVA TS 5130MM
200 um
Vega ©Tescan
Digital Microscopy Imaging

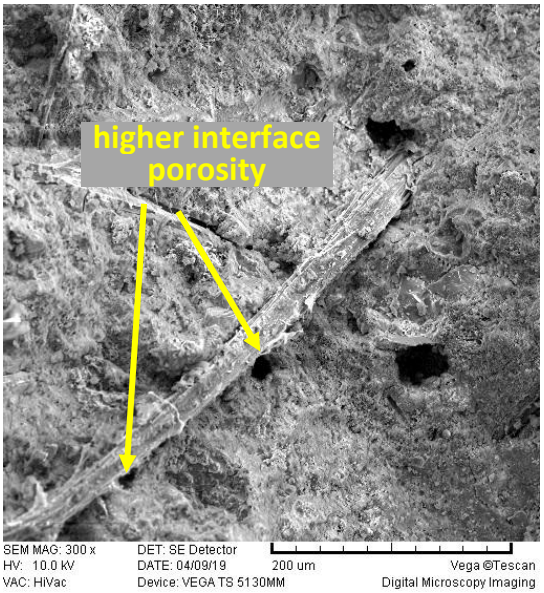
higher interface
porosity
SEM MAG: 300 x
HV: 10.0 kV
VAC: HiVac
DET: SE Detector
DATE: 04/09/19
Device: VEVA TS 5130MM
200 um
Vega ©Tescan
Digital Microscopy Imaging

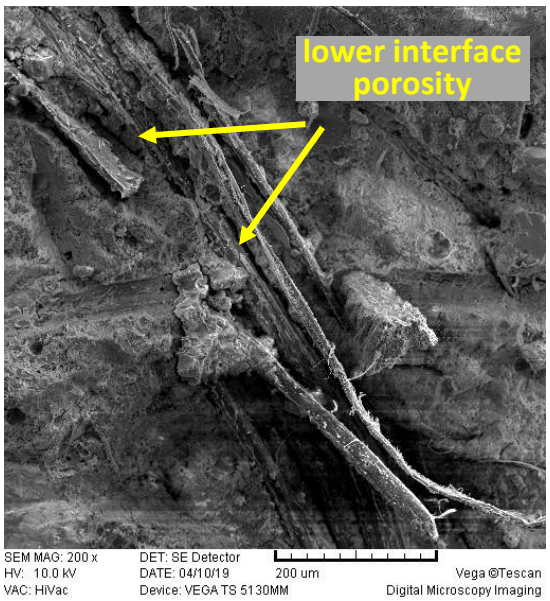
lower interface
porosity
SEM MAG: 200 x
HV: 10.0 kV
VAC: HiVac
DET: SE Detector
DATE: 04/10/19
Device: VEVA TS 5130MM
200 um
Vega ©Tescan
Digital Microscopy Imaging

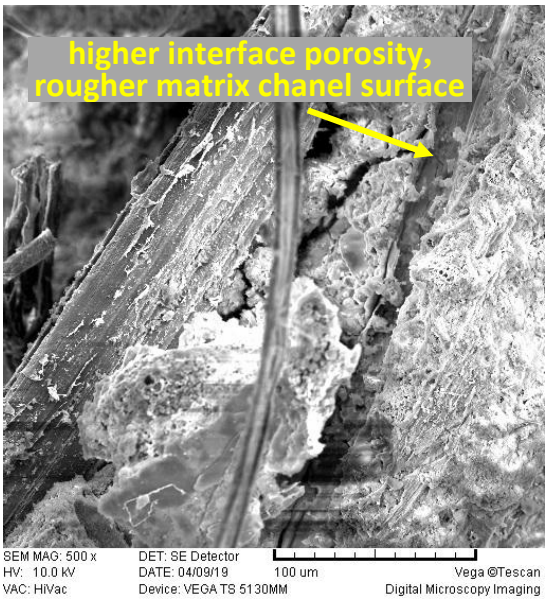
higher interface porosity,
rougher matrix chanel surface
SEM MAG: 500 x
HV: 10.0 kV
VAC: HiVac
DET: SE Detector
DATE: 04/09/19
Device: VEVA TS 5130MM
100 um
Vega ©Tescan
Digital Microscopy Imaging

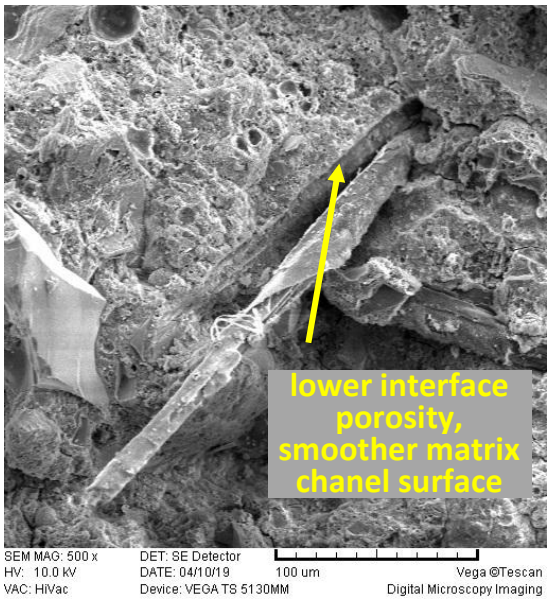
lower interface
porosity,
smoother matrix
chanel surface
SEM MAG: 500 x
HV: 10.0 kV
VAC: HiVac
DET: SE Detector
DATE: 04/10/19
Device: VEVA TS 5130MM
100 um
Vega ©Tescan
Digital Microscopy Imaging

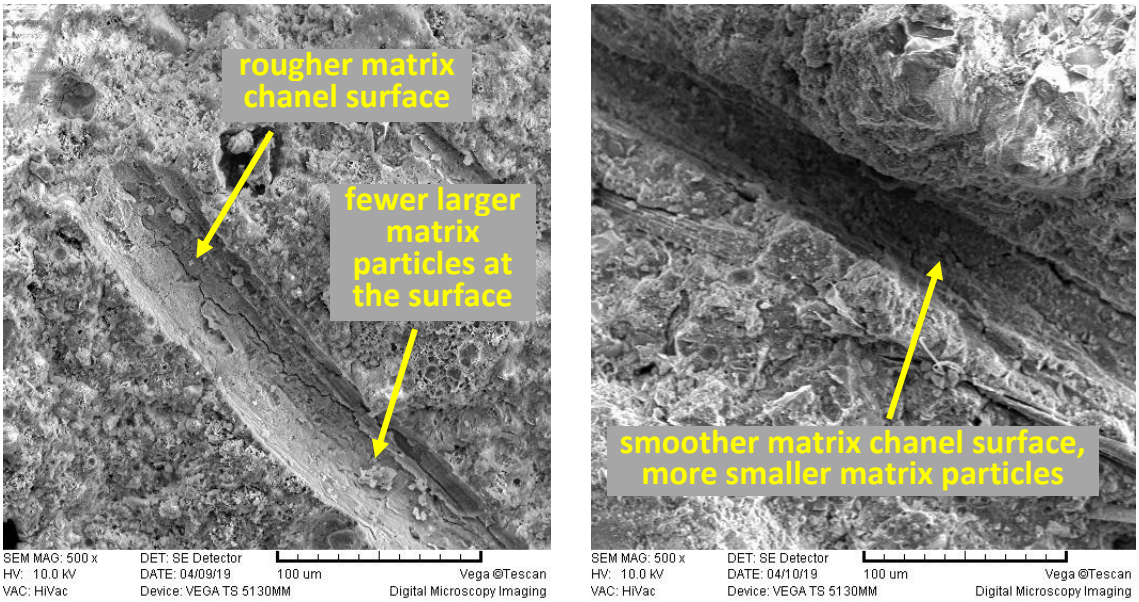

Figure 13. SEM images of fracture surfaces of AA mortars (1.0 vol% of hemp fibres) with fibre/matrix interface and the matrix channel after fibres pull-out: a) fly ash based AA mortar - FA1_1.0 (left) ; b) fly ash and GGBFS based AA mortar - FA2S_1.0 (right)

Conclusion

In this research, the physical, mechanical and microstructural properties of AA mortars (containing fine aggregates of particle size 0.0-4.0 mm) reinforced with short discrete hemp fibres (0.5 vol% and 1.0 vol% dosages; 10 mm in length) were evaluated. Two different series of AA mortar matrices based on different solid prime materials were used.

The first AA mortar (FA1) contained only fly ash and had lower density with higher porosity (was less compact) than the second AA mortar (FA2S) that contained a combination of fly ash and ground granulated blast furnace slag (GGBFS). The FA2S mortar had 48% higher compressive strength, with 5% lower flexural strength and was more brittle (had 17% lower energy absorption capacity under flexure) than the less compact FA1 mortar.

Based on the results of this research, with the addition of hemp fibres to these mortars, it could be concluded that:

- the density of both mortar series slightly decreases (up to 5%) irrespectively from the fibre dosage;
- the water absorption rate of FA2S mortar increases by 15% and 20% (for 0.5 vol% and 1.0 vol% fibre dosage), whereas in FA1 series it increases up to 23%, irrespectively from the fibre dosage;
- the compressive strength of both mortar series only slightly change (up to 10%) irrespectively from the fibre dosage;
- the flexural strength of FA1 series decreases by 7% and 21% (for 0.5 vol% and 1.0 vol%). By FA2S series it remains almost constant;
- by both mortar series the energy absorption capacity under flexure significantly increases, i.e. with the increasing dosage of fibres up to 134% and 266%. However, in FA2S series (the initially more brittle plain matrix) there is a significantly higher (2 times) relative energy absorption capacity increase with the addition of hemp fibres than in the FA1 matrix. Due to its smaller particle sizes, the FA2S matrix is denser with lower porosity that in turn results in a lower fibre/matrix interface porosity and smoother fibre/matrix interface (with lower surface asperity). Consequently, in FA2S matrix way more fibre/matrix contact points exist than in FA1 matrix that ensures a stronger (more optimal) fibre/matrix interfacial bond- and frictional resistance.

As a result of their significant energy absorption capacity combined with good compression and flexural strength, hemp fibre AA mortars could be a potential replacement for traditional cementitious mortars in applications where high toughness and crack resistance is needed, i.e. hinge area of clamped columns or cores of buildings which are generally designed to sustain high lateral (seismic or wind) loads.

However, hemp fibre mortars based on a combination of fly ash and ground granulated blast furnace slag of this study are expected to have a better long term performance compared to fly ash based mortars since, in terms of durability the compactness, density and porosity of the composite plays a decisive role.

Acknowledgements

The authors greatly acknowledge the financial support provided by the Federal Ministry of Science, Research and Economy (BMWFW) in Austria, Ministry of Education, Youth and Sports of the Czech Republic and the Ministry of Education, Science and Technological Development of the Republic of Serbia (projects TR 34026 and TR36017) in the frame of Multilateral S&T Cooperation Program in the Danube Region for the research project "*Fiber-reinforced alkali-activated composites (properties and selected durability aspects)*" under the grant nr. MULT_DR 08/2017. The authors would like to thank Dr. Nataša Džunuzović (Institute for Multidisciplinary Research, University of Belgrade) for assistance in acquiring the SEM data.

References

[1] L. Huang, G. Krigsvoll, F. Johansen, Y. Liu, X. Zhang, Carbon emission of global construction sector, Renewable and Sustainable Energy Reviews. 81 (2018)

[2] S. Amziane, F. Collet, eds., Bio-aggregates Based Building Materials, State-of-the-Art Report of the RILEM Technical Committee 236-BBM, (2017)

[3] A. Bilodeau, V.M. Malhotra, High-Volume Fly Ash System: Concrete Solution for Sustainable Development, Materials Journal. 97 (2000) 41–48.

[4] E. Cohen, A. Peled, G. Bar-Nes, Dolomite-based quarry-dust as a substitute for fly-ash geopolymers and cement pastes, Journal of Cleaner Production. 235 (2019) 910–919.

[5] B. Ilić, V. Radonjanin, M. Malešev, M. Zdujić, A. Mitrović, Study on the addition effect of metakaolin and mechanically activated kaolin on cement strength and microstructure under different curing conditions, Construction and Building Materials. 133 (2017) 243–252.

[6] J. Davidovits, False Values on CO2 Emission for Geopolymer Cement / Concrete published in Scientific Papers The Manufacture of Geopolymer Cement / Concrete, Geopolymer Institute Library. (2015) 1–9.

[7] I. Ismail, S.A. Bernal, J.L. Provis, R. San Nicolas, D.G. Brice, A.R. Kilcullen, S. Hamdan, J.S.J. Van Deventer, Influence of fly ash on the water and chloride permeability of alkali-activated slag mortars and concretes, Construction and Building Materials. 48 (2013) 1187–1201.

[8] M. Nedeljković, B. Šavija, Y. Zuo, M. Luković, G. Ye, Effect of natural carbonation on the pore structure and elastic modulus of the alkali-activated fly ash and slag pastes, Construction and Building Materials. 161 (2018) 687–704.

[9] J.L. Provis, Alkali-activated materials, Cement and Concrete Research. 114 (2018) 40–48.

[10] J.L. Provis, J.S.J. van Deventer, 16 - Geopolymers and Other Alkali-Activated Materials, in: Lea's Chemistry of Cement and Concrete (Fifth Edition), (2019).

[11] M. Komljenovic, Mechanical strength and Young's modulus of alkali-activated cement-based binders, in: Handbook of Alkali-Activated Cements, Mortars and Concretes, (2015), pp. 171–215.

[12] J.R. Yost, A. Radlińska, S. Ernst, N.J. Martignetti, Structural Behavior of Alkali Activated Fly Ash Concrete. Part 2: Structural Testing and Experimental Findings, Materials and Structures. 46 (2012) 449–462.

[13] J.R. Yost, A. Radlińska, S. Ernst, M. Salera, Structural Behavior of Alkali Activated Fly Ash Concrete. Part 1: Mixture Design, Material Properties and Sample Fabrication, Materials and Structures. 46 (2012) 435–447.

[14] I. Garcia-Lodeiro, A. Palomo, A. Fernández-Jiménez, 2 - An overview of the chemistry of alkali-activated cement-based binders, in: Handbook of Alkali-Activated Cements, Mortars and Concretes, (2015) pp. 19–47.

[15] A. Bentur, S. Mindess, Fibre Reinforced Cementitious Composites, Modern Concrete Technology Series. (1990).

[16] C. Johnston, Fiber-Reinforced Cements and Concretes (Advances in Concrete Technology), (2000).

[17] B. Mobasher, Fibre-reinforced concrete: From design to structural applications, (2014).

[18] B. Prabu, A. Shalini, Behaviour of Fibre Reinforced Geopolymer Mortar, (2016).

[19] B. Nematollahi, J. Qiu, E.-H. Yang, J. Sanjayan, Microscale investigation of fiber-matrix interface properties of strain-hardening geopolymer composite, Ceramics International. 43 (2017).

[20] A. Islam, U.J. Alengaram, M.Z. Jumaat, N.B. Ghazali, S. Yusoff, I.I. Bashar, Influence of steel fibers on the mechanical properties and impact resistance of lightweight geopolymer concrete, Construction and Building Materials. 152 (2017) 964–977.

[21] H. Savastano Jr., P.G. Warden, R.S.P. Coutts, Mechanically pulped sisal as reinforcement in cementitious matrices, Cement and Concrete Composites. 25 (2003) 311–319.

[22] R.D. Tolêdo Filho, K. Ghavami, G.L. England, K. Scrivener, Development of vegetable fibre-mortar composites of improved durability, Cement and Concrete Composites. 25 (2003) 185–196.

[23] R.D. Tolêdo Filho, K. Scrivener, G.L. England, K. Ghavami, Durability of alkali-sensitive sisal and coconut fibres in cement mortar composites, Cement and Concrete Composites. 22 (2000) 127–143.

[24] F.D.A. Silva, B. Mobasher, C. Soranakom, R.D.T. Filho, Effect of fiber shape and morphology on interfacial bond and cracking behaviors of sisal fiber cement based composites, Cement and Concrete Composites. 33 (2011) 814–823.

[25] F.D.A. Silva, R. Dias, T. Filho, J. De Almeida, M. Filho, E. De Moraes, R. Fairbairn, Physical and mechanical properties of durable sisal fiber – cement composites, Construction and Building Materials. 24 (2010) 777–785.

[26] E.K. Tschegg, A. Schneemayer, I. Merta, K.A. Rieder, Energy dissipation capacity of fibre reinforced concrete under biaxial tension-compression load. Part I: Test equipment and work of fracture, Cement and Concrete Composites. 62 (2015) 195–203.

[27] E.K. Tschegg, A. Schneemayer, I. Merta, K.A. Rieder, Energy dissipation capacity of fibre reinforced concrete under biaxial tension-compression load. Part II: Determination of the fracture process zone with the acoustic emission technique, Cement and Concrete Composites. 62 (2015) 187–194.

[28] R. De Souza, L. Maria, S. De Souza, F. De Andrade, Comparative study on the mechanical behavior and durability of polypropylene and sisal fiber reinforced concretes, Construction and Building Materials. 211 (2019) 617–628.

[29] M. Ernestina, A. Fidelis, R. Dias, T. Filho, F.D.A. Silva, B. Mobasher, S. Müller, V. Mechtcherine, C. Engineering, U. Federal, P.O. Box, C.E.P.R. De Janeiro, Interface characteristics of jute fiber systems in a cementitious matrix, Cement and Concrete Research. 116 (2019) 252–265.

[30] I. Merta, A. Mladenovič, J. Turk, A. Šajna, M. Pranjić, Life Cycle Assessment of Natural Fibre Reinforced Cementitious Composites, 6th International Conference on Non-Traditional Cement and Concrete, Brno, Czech Republic; (19.06.2017 - 22.06.2017).

[31] I. Merta, A. Šajna, B. Poletanovic, A. Mladenović, Influence of natural fibres on mechanical properties and durability of cementitious mortars, CoMS - 1st International Conference on Construction Materials for Sustainable Future, Zadar; (19.04.2017 - 21.04.2017).

[32] S.R.D. Petroudy, 3 - Physical and mechanical properties of natural fibers, Elsevier Ltd, 2017.

[33] L. Yan, B. Kasal, L. Huang, A review of recent research on the use of cellulosic fibres, their fibre fabric reinforced cementitious, geo-polymer and polymer composites in civil engineering, Composites Part B. 92 (2016) 94–132.

[34] M. Alzeer, K.J.D. Mackenzie, Synthesis and mechanical properties of new fibre-reinforced composites of inorganic polymers with natural wool fibres, Journal of Materials Science. (2012) 6958–6965.

[35] R.G. Elenga, G.F. Dirras, J.G. Maniongui, P. Djemia, M.P. Biget, Composites : Part A On the microstructure and physical properties of untreated raffia textilis fiber, Composites Part A. 40 (2009) 418–422.

[36] A.P. Fantilli, S. Sicardi, F. Dotti, Virtual Special Issue Bio Based Building Materials The use of wool as fiber-reinforcement in cement-based mortar, Construction and Building Materials. 139 (2017) 562–569.

[37] S. G., Bergström, H.E. Gram, Durability of alkali-sensitive fibres in concrete, International Journal of Cement Composites and Lightweight Concrete, Volume 6, Issue 2, (1984) pp. 75-80

[38] C. Juárez , A. Durán, P. Valdez, G. Fajardo, Performance of "Agave lecheguilla" natural fiber in portland cement composites exposed to severe environment conditions, Building and Environment, 42, (2007) pp. 1151-1157.

[39] A. Kriker, A. Bali, G. Debicki, M. Bouziane, M. Chabannet, Durability of date palm fibres and their use as reinforcement in hot dry climates", Cement & Concrete Composites, 30, (2008) pp. 639-648

[40] M. Troëdec, C.S. Peyratout, A. Smith, T. Chotard, Influence of various chemical treatments on the interactions between hemp fibres and a lime matrix. J. Eur. Ceram. Soc. 29, (2009) 1861–1868.

[41] I. Merta, K. Kopecsko , E. Tschegg, Durability of hemp fibers in the alkaline environment of cement matrix, Fibre Reinforced Concrete: challenges and opportunities, 8th Tilem International Symposium on fibre reinforced concrete (BEFIB 2012), Guimarães, Portugal

[42] J. A. M. Filho, F.A. Silva, R.D. Toledo Filho, Degradation kinetics and aging mechanisms on sisal fiber cement composite systems, Cement and Concrete Composites, Volume 40, (2013) pp 30-39

[43] J. Wei and C. Meyer, Degradation mechanisms of natural fiber in the matrix of cement composites, Cement and Concrete Research 73 (2015) 1–16

[44] J. Wei and C. Meyer, Degradation of natural fiber in ternary blended cement composites containing metakaolin and montmorillonite, Corrosion Science, Volume 120, (2017) pp. 42-60

[45] I. Merta, B. Poletanovic, K. Kopecsko, Durability Of Natural Fibres Within Cement-Based Materials - Review; Concrete Structures. Journal of the Hungarian Group of fib (Federation International de Beton), **18** (2017), S. 10 - 16.

[46] F. Amalia, N. Akihaf, Nurfadilla, Subaer, Development of Coconut Trunk Fiber Geopolymer Hybrid Composite for Structural Engineering Materials, in: Materials Science and Engineering, (2017).

[47] K. Korniejenko, E. Frączek, E. Pytlak, M. Adamski, Mechanical Properties of Geopolymer Composites Reinforced with Natural Fibers, in: Procedia Engineering, (2016): pp. 388–393.

[48] T. Alomayri, I.M. Low, Synthesis and characterization of mechanical properties in cotton fiber-reinforced geopolymer composites, Journal of Asian Ceramic Societies. 1 (2013) 30–34.

[49] T. Alomayri, F.U.A. Shaikh, I.M. Low, Characterisation of cotton fibre-reinforced geopolymer composites, Composites: Part B. 50 (2013) 1–6.

[50] R. Chen, S. Ahmari, L. Zhang, Utilization of sweet sorghum fiber to reinforce fly ash-based geopolymer, Journal of Materials Science. 49 (2014) 2548–2558.

[51] R.A. Sá Ribeiro, M.G. Sá Ribeiro, K. Sankar, W.M. Kriven, Geopolymer-bamboo composite – A novel sustainable construction material, Construction and Building Materials. 123 (2016) 501–507.

[52] E.A.S. Correia, S.M. Torres, K.C. Gomes, N. P. Barbosa, Mechanical Performance of Natural Fibers Reinforced Geopolymer Composites, Materials Science Forum. 758 (2013) 139–145.

[53] R.A.J. Malenab, J.P.S. Ngo, M.A.B. Promentilla, Chemical Treatment of Waste Abaca for Natural Fibre-Reinforced Geopolymer Composite, Materials. (2017).

[54] T. Alomayri, F.U.A. Shaikh, I.M. Low, Effect of fabric orientation on mechanical properties of cotton fabric reinforced geopolymer composites, Materials and Design. 57 (2014) 360–365.

[55] T. Alomayri, H. Assaedi, F.U.A. Shaikh, I.M. Low, Effect of water absorption on the mechanical properties of cotton fabric-reinforced geopolymer composites, Journal of Asian Ceramic Societies. 2 (2014) 223–230.

[56] H. Assaedi, F.U.A. Shaikh, I.M. Low, Effect of nanoclay on durability and mechanical properties of flax fabric reinforced geopolymer composites, Journal of Asian Ceramic Societies. 5 (2017) 62–70.

[57] H. Assaedi, F.U.A. Shaikh, I.M. Low, Characterizations of flax fabric reinforced nanoclay-geopolymer composites, Composites Part B. 95 (2016) 412–422.

[58] S.S. Musil, Green composite: sodium-based geopolymer reinforced with chemically extracted corn husk fibres, Developments in Strategic Materials and Computational Design IV. (2014) 123–133.

[59] A.C.C. Trindade, P.H.R. Borges, F. de Andrade Silva, Mechanical behavior of strain-hardening geopolymer composites reinforced with natural and PVA fibers, Materials Today: Proceedings. 8 (2019) 753–759.

[60] A. Teixeira-pinto, B. Varela, K. Shrotri, R.S.P. Panandiker, J. Lawson, Geopolymer-jute composite: A novel environmentally friendly composite with fire resistant properties, The American Ceramic Society. (2008) 337–345.

[61] M. Alshaaer, S.A. Mallouh, J. Al-Kafawein, Y. Al-faiyz, T. Fahmy, A. Kallel, F. Rocha, Fabrication, microstructural and mechanical characterization of Luffa Cylindrical Fibre - Reinforced geopolymer composite, Applied Clay Science. 143 (2017) 125–133.

[62] M. Alzeer, K. Mackenzie, Synthesis and mechanical properties of novel composites of inorganic polymers (geopolymers) with unidirectional natural flax fibres (phormium tenax), Applied Clay Science. 75–76 (2013) 148–152.

[63] M. Alzeer, K.J.D. Mackenzie, Synthesis and mechanical properties of new fibre-reinforced composites of inorganic polymers with natural wool fibres, Journal of Materials Science. (2012) 6958–6965.

[64] T. Alomayri, F.U.A. Shaikh, I.M. Low, Synthesis and mechanical properties of cotton fabric reinforced geopolymer composites, Composites Part B: Engineering. 60 (2014) 36–42.

[65] N. Ranjbar, M. Zhang, Fiber-reinforced geopolymer composites: A review, Cement and Concrete Composites, Volume 107, (2020) ,10349

[66] ASTM C618. 2015. 'Standard Specification for Coal Fly Ash and Raw or Calcined Natural Pozzolan for Use in Concrete'. West Conshohocken, Pennsylvania., (2015).

[67] CEN. 2012. EN 450-1: Fly Ash for Concrete — Part 1: Definition, Specifications and Conformity Criteria. Brussels: European Committee for Standardization., (2012).

[68] M.Jawaid, H.P.S.Abdul Khalil, Cellulosic/synthetic fibre reinforced polymer hybrid composites: A review, Carbohydrate Polymers 86 (2011) 1– 18

[69] M. Komljenović, Z. Baščarević, V. Bradić, Mechanical and microstructural properties of alkali-activated fly ash geopolymers, Journal of Hazardous Materials. 181 (2010) 35–42.

[70] CEN, Brussels. 2008. 'EN 196-1: Methods of Testing Cement - Part 1: Determination of Strength'. Brussels., (2008).

[71] ÖNORM EN 1015-11: 2018 01 01, Methods of test for mortar for masonry - Part 11: Determination of flexural and compressive strength of hardened mortar, (2018).

[72] Z.P. Bazant, J. Planas, Fracture and Size Effect in Concrete and Other Quasibrittle Materials, Published December 29, 1997 by CRC Press, ISBN 9780849382840

[73] G.M.J. Van Mier, Concrete Fracture: A Multiscale Approach, 2012, ISBN 978-1-4665-5470-2

[74] Z. Li, S. Liu, Influence of Slag as Additive on Compressive Strength of Fly Ash-Based Geopolymer, , Journal of Materials in Civil Engineering, Volume 19, (2007) Issue 6

[75] Z. Zhang, H. Wang, 9-Analysing the relation between pore structure and permeability of alkali-activated concrete binders, 2 - An overview of the chemistry of alkali-activated cement-based binders, in: Handbook of Alkali-Activated Cements, Mortars and Concretes, (2015) pp. 235–262.

[76] Z. Li, W. Xungai, W. Lijing, Properties of hemp fibre reinforced concrete composites, Composites Part A: Applied Science and Manufacturing. 37 (2006) 497–505.

[77] J. Page, F. Khadraoui, M. Gomina, M. Boutouil, Influence of different surface treatments on the water absorption capacity of flax fibres: Rheology of fresh reinforced-mortars and mechanical properties in the hardened state, Construction and Building Materials. 199 (2019) 424–434.

[78] M. Ardanuy, J. Claramunt, R.D. Toledo Filho, Cellulosic fiber reinforced cement-based composites: A review of recent research, Construction and Building Materials. 79 (2015) 115–128.

[79] K. Sankar, R.A. Sá Ribeiro, M.G. Sá Ribeiro, W.M. Kriven, P. Colombo, Potassium-Based Geopolymer Composites Reinforced with Chopped Bamboo Fibers, Journal of the American Ceramic Society. 100 (2017) 49–55.

[80] E. Rill, D. R. Lowry and W. M. Kriven, Properties of basalt fiber reinforced geopolymer composites, Conference: 34th International Conference & Exposition on Advanced Ceramics & Composites, 2010

[81] B. Poletanovic, I. Merta, A. Sajna, A. Mauko Pranjic, A. Mladenovic, Comparison Of Physical And Mechanical Properties Of Cementitious Mortars Reinforced With Natural And Synthetic Fibres Prior And After Wet/dry Cycles, ICBBM 2019 3th International Conference On Bio-Based Building Materials, Belfast, UK; 26.06.2019 - 28.06.2019; in: "Proceedings of the 3th International Conference On Bio-Based Building Materials", (2019), pp 433 - 437.